Genetic dissection of epistatic and QTL by environment interaction effects in three bread wheat genetic backgrounds for yield-related traits under saline conditions

Mojtaba Jahani · Ghasem Mohammadi-Nejad · Babak Nakhoda · Loren H. Rieseberg

Abstract Salt stress represents a major impediment to global wheat production. Development of wheat varieties that offer tolerance to salt stress would increase productivity. Here we report on the results of a genetic study of salt tolerance in bread wheat across multiple genetic backgrounds and environments, with the goal of identifying quantitative trait loci (QTLs) for 9 yield-related traits that are both genetic background independent and environmentally stable. Three RIL populations derived from crosses between a super salt tolerant landrace (Roshan) and 3 bread-wheat cultivars (Falat, Sabalan, Superhead#2) that vary in salt tolerance were phenotyped in three environments. Genetic maps were constructed for each RIL population and independent analyses of each population/environment combination revealed significant associations of 92 genomic regions with the traits evaluated. Joint analyses of yield-related traits across all populations revealed a strong genetic background effect, with no QTLs shared across all genetic backgrounds. Fifty-seven QTLs identified in the independent analysis co-localized with those in the joint analysis. Overall, only 3 QTLs displayed significant epistatic interactions. Additionally, a total of 67 QTLs were identified in QTL analysis across environments, two of these (QSPL.3A, QBYI.7B-1) were both stable and not reported previously. Such novel and stable QTLs may accelerate marker-assisted breeding of new highly productive and salt tolerant bread-wheat varieties.

M. Jahani · G. Mohammadi-Nejad (✉)
Department of Agronomy and Plant Breeding, College of Agriculture, Shahid-Bahonar University of Kerman, P.O.B. 76169-133, Kerman, Iran
e-mail: mohammadinejad@uk.ac.ir

B. Nakhoda
Department of Molecular Physiology, Agricultural Biotechnology Research Institute of Iran, Research, Education and Extension Organization (AREEO), Karaj, Iran

L. H. Rieseberg
Department of Botany and Beaty Biodiversity Centre, University of British Columbia, Vancouver, BC V6T 1Z4, Canada

Introduction

Bread wheat (*Triticum aestivum*) is a globally important crop, providing approximately 30% of global grain production, and 20% of total calories and plant-derived protein for the world's population (FAO 2018). To

meet expected food requirements of wheat-consuming countries over the next half century, it is estimated that wheat production must increase by approximately 70% (Ray et al. 2012). According to the FAO, salinity stress is a major constraint to agricultural food production generally and to wheat specifically. Salinity stress reduces yields and limits the use of agricultural land. Given that around 20% of all agricultural land is salinated, the development of salt tolerant crop varieties would contribute importantly to food security.

Salinity can have several different negative effects on plant growth and reproduction, including reductions in water availability, ion toxicity, and induction of nutrient deficiencies. As a consequence, plant responses to salinity stress are typically genetically and physiologically complex, involving the interaction of many gene pathways, as well as the environment (Flowers and Flowers 2005). Hence, not only is the identification and molecular characterization of salinity stress related quantitative trait loci (QTLs) critical for accelerating marker-aided breeding of salt tolerant crops, but also such QTL analyses are most likely to be successful if conducted under multiple environments with the varying degrees of stress (Mathews et al. 2008).

Multi-environment trials (METs) are often used to evaluate the performance of genotypes across sites and years. If the interest is exclusively in phenotypic variation, then a panel that maximizes crop diversity is typically employed. However, if genetic information is wanted as well, then METs for bi-parental populations are routinely examined, since they enable detection of QTLs and their interactions with each other and the environment. Examples include a recent study of 150 recombinant inbred lines (RILs) of maize to evaluate three ear-leaves area across multi-environments via inclusive composite interval mapping (Cui et al. 2017). Similarly, a doubled haploid population of 222 lines was characterized with 182 markers and grown in multi-environments to dissect QTL by environment interactions for grain yield components in winter wheat (Zheng et al. 2010). With sufficient marker density, one can conduct genetic analyses in more complex populations for genetic analyses, such as NAM or MAGIC populations, or diversity panels. Such association mapping population approaches have the advantage of sampling many more alleles underlying traits of interest, but are less powerful for assessing interactions among alleles at within or among loci.

Interactions between non-allelic genes (epistasis) have become an increasingly important focus of QTL studies since epistatic interactions appear to especially frequent for performance related traits such as plant height and yield. For example, Zhang et al. (2008) conducted a series of trials in which they found a significant epistatic effect for plant height in a population of doubled haploid wheat. Epistatic interactions can be important for morphological and developmental traits as well, such as kernel morphometric traits (Prashant et al. 2012) and coleoptile growth in wheat (Rebetzke et al. 2007).

Another major difficulty of marker-assisted breeding projects is the genetic background (GB) effect. GB impedes general utilization of QTLs identified in different backgrounds. Several studies have revealed that GB acts on the expression of QTL for yield and its components (Yao et al. 2016; Venuprasad et al. 2012; Prashant et al. 2012; Wei et al. 2009; Han et al. 2012;Wang et al. 2014; Vikram et al. 2011).

Whereas some research has been carried out on wheat QTL mapping for salinity stress, there have been few empirical investigations into main, epistatic, environment and genetic background effects in one comprehensive experiment. In this study, three RIL populations with diverse salinity tolerance and genetic backgrounds (Roshan × Falat, Roshan × Sabalan and Roshan × Superhead#2) were used to discover genomic regions underlying phenotypic variation in yield-related traits under salinity stress. The three RIL populations were evaluated across distinct environments that varied in salinity stress. The major objectives of this study were to (1) detect QTLs for morphological traits and grain yield-related traits under salinity stress in each genetic background and environment; (2) evaluate whether GB affects the identification and expression of QTLs; (3) investigate epistatic effects among detected QTLs; and (4) examine QTL by environment effects and find the most stable QTLs across different environments.

Materials and methods

Plant materials and DNA extraction

Three RIL mapping populations were derived from crosses between a common parent, Roshan (tolerant to salinity stress, tall, landrace) and three different

parents: (1) Falat (highly sensitive to salinity stress, high grain yield, dwarf, cultivar); (2) Sabalan (sensitive to salinity stress, high grain yield, tall, cultivar); and (3) Superhead#2 (highly sensitive to salinity stress, high grain yield, dwarf, cultivar). The common parent Roshan has been reported as a salt tolerant landrace in several salinity stress experiments (Poustini and Siosemardeh 2004; Dehdari et al. 2005). All the crosses were carried out in 2003. Roshan*Falat (RF), Roshan*Sabalan (RS) and Roshan*Superhead#2 (RSH) RIL populations contain 313, 254 and 186 genotypes, respectively. They were developed by single seed descent at the Agricultural Biotechnology Research Institute of Iran in 2010 (ABRII, Karaj, Iran) (Supplementary Figure 1). 100 mg leaf tissue of each RIL was collected from seedlings for extraction of high-quality genomic DNA following the Triticarte plant DNA extraction protocol (http://www.triticarte.com.au/content/DNA-preparation.html). Extracted DNA was adjusted to a concentration of 50 ng/μl for marker analysis.

Genetic linkage map

Genomic DNA of RF, RS and RSH RIL populations were subjected to Diversity Arrays Technology (DArT) genome profiling (Akbari et al. 2006; Wenzl et al. 2004) at Triticarte Pty Ltd, Australia (http://www.triticarte.com.au) (raw data is available in Supplementary Data). DArT generates whole-genome fingerprints in a single microarray-based assay by scoring the presence versus absence of DNA fragments in genomic representations generated from samples of genomic DNA (Akbari et al. 2006). Polymorphic markers were used to construct the linkage map using QTL IciMapping software version 4.1 (http://www.isbreeding.net) and the Kosambi mapping function (Kosambi 1943). Heterozygous loci were considered as missing data and the threshold for the likelihood of odds (LOD) ratio was set to 3.0.

Field trials and trait evaluation

The 313, 254 and 186 genotypes within each RIL population were evaluated in three different environments; Kerman in 2012, Kerman in 2013 (30°20′ N and 56°54′ E) and Yazd in 2011 (32°30′ N and 54°05′ E), all of which were sufficiently saline (electrical conductivity values of > 4 dS m^{-1}) to produce deleterious effects on wheat (McFarland et al. 2014). Field experiments were carried out in homogenized salinity plots at CEAS (Center of Excellence for Abiotic stresses in Cereals). Electrical conductivity (EC) values in the Kerman experimental field were 12.5 and 10 dS m^{-1} for soil and for irrigation water, respectively. Similarly, EC values of 10.5 and 9 dS m^{-1} were recorded for soil and for irrigation water, respectively, in Yazd. RF, RS and RSH in Kerman-2013 and RF, RS in Kerman-2012 were seeded in an incomplete block design (lattice) with two replications while all three RIL populations in Yazd-2011 experiment and RSH in Kerman-2012 experiment were laid out with an augmented design. In the augmented design, sets of 20 lines were assigned randomly to a block with 3 check cultivars (Arg, Bam, Kavir). Field trial characteristics and traits evaluated are highlighted in Table 1. In all experiments, plots were 200 cm long and six rows wide, with 20 cm spaces between rows and 10 cm between two plants in a row. The experiments were carried out during the local wheat-growing season (November–May). Weather data was collected from the nearest weather station for each experiment and summarized in Supplementary Figure 2. Standard agronomic practices were carried out to minimize weed and insect damage in order to reach maximum grain yield. The 4 center rows of each plot were used to collect data for plant height (PHT, measured from the soil surface to the tip of the tallest spike), spike length (SPL), spike weight (SPW), spikes per plant (SPP), weight of kernels per plant (WKP), thousand kernel weight (TKW, kernel weight was measured based on 100 kernels and converted to 1000-kernal weight), biological yield per m^2 (BYI), grain yield per m^2 (GYLD, determined as the average weight of bulked harvested grain per square meter) and harvest index (HAI) (Grain weight/Total biomass) in the RF population. In the RS population PHT, SPL, SPW, TKW, BYI, GYLD and HAI were measured. Lastly, in the RSH population PHT, SPL, TKW and GYLD were evaluated. Five randomly chosen plants from 4 central rows of each plot were phenotyped for PHT, SPL, SPW, SPP, WKP and TWK. The values were averaged and used as the measurements for the plot. BYI, GYLD and HAI were evaluated based on one central square meter. Experimental error was calculated based on the replicated checks in the augmented design and used to calculate adjusted genotype means for blocks.

Table 1 A summary of field trials and evaluated traits

Year	Location	Electrical conductivity (dS m^{-1})		Population	Experimental design	Evaluated traits								
		Water	Soil			PHT	SPL	SPW	SPP	WKP	TKW	BYI	GYLD	HAI
2011	Yazd	9	10.5	RF	Augmented design[a]	*	*	*	*	*	*	*	*	*
				RS	Augmented design[a]	*	*	*			*	*	*	*
				RSH	Augmented design[a]	*	*				*		*	
2012	Kerman	10	12.5	RF	Incomplete block design	*	*	*	*	*	*	*	*	*
				RS	Incomplete block design	*	*	*			*	*	*	*
				RSH	Augmented design[a]	*	*				*		*	
2013	Kerman	10	12.5	RF	Incomplete block design	*	*	*	*	*	*	*	*	*
				RS	Incomplete block design	*	*	*			*	*	*	*
				RSH	Incomplete block design	*	*				*		*	

[a]Arg, Bam and Kavir were cultivars used as check in augmented design

However, the PROC LATTICE procedure in SAS (SAS Institute, version 9.1.3) was used to calculate adjusted means for lattice design experiments. Adjusted values of each trait were used for QTL mapping, except that square root normalizing transformations were performed on GYLD (in RF, RS and RSH), BYI (in RF and RS) and SPL (in RF and RSH).

QTL mapping

Main additive QTLs (M-QTLs) in each environment and genetic background were identified by the method of inclusive composite interval mapping (ICIM) by QTL IciMapping version 4.1 (Li et al. 2008). Scanning step and the PIN (*P* value for entering variables) values were set at 5 and 0.01, respectively. Chromosomal regions with LOD ≥ 3.0 were considered as significant M-QTLs.

ICIM epistatic interaction analysis was used to find possible epistatic interactions among detected M-QTLs. Genomic regions with LOD value ≥ 5.0 were declared as significant epistatic QTLs (E-QTLs).

The multi-environment trials (MET) function in QTL IciMapping version 4.1 was employed to detect QTL by environment interactions across all environments in each genetic background. QTLs with LOD scores ≥ 3.0 were selected for QTL stability analysis.

All QTLs were labeled in a precise fashion. The QTL identification labels break down as follows: An uppercase 'Q' signifies 'QTL'; the letters following the Q and prior to the period are an abbreviation of a specific corresponding trait; followed by the wheat chromosome of the corresponding QTL. Lastly, QTLs that have more than one locus in the same chromosome are defined by a numerical value that is further separated by a dash. M-QTLs and QTLs that were detected in multi-environment trials were labeled separately.

To clarify the pattern of QTL stability, a biplot methodology was used. PCA was performed on QTL by environment interaction effects. The first principal component score (absolute value) for each QTL was plotted against its absolute additive effect value. QTLs with absolute additive effects greater than the additive by environment effects are considered stable QTLs (Li et al. 2015).

Results

Evaluation of phenotypic traits revealed a wide range of phenotypic variation. Significant differences were observed among RILs for most of the traits in each environment (data not shown). Descriptive statistics (maximum, minimum, standard deviation and mean value) of evaluated traits for different populations and environments are presented in Table 2. For example, the lowest grain yield was 2.72 g/m^2 and the highest was 664 g/m^2 in RF Kerman-2013 and RSH Kerman-2012, respectively. In addition, the shortest genotype was found in RS Kerman-2012 (15.41 cm) and the tallest in RSH Kerman-2012 (94.5 cm). Furthermore, spike length of the RF population ranged from 4.8 to 11.1 cm in Kerman-2013, while RSH population spike length ranged from 3.6 to 27 cm in Kerman-2012. In the majority of environments, the maximum values of each trait were vastly larger than the minimum values. All evaluated traits displayed continuous phenotypic variation in all environments, consistent with polygenic inheritance (Supplementary Figure 3).

Construction of linkage maps

RF, RS, RSH populations were genotyped with 2605, 2717 and 868 DArT markers, respectively. Linkage analysis was carried out after excluding redundant or monomorphic markers from the data set. DArT markers were genetically mapped to 21 linkage groups based on anchor information received from Triticarte (http://www.diversityarrays.com) and linkage analysis at LOD 3.0. In the RF population, a total of 810 polymorphic markers, spanning a total length of 6095.88 cM with an average density of one marker per 7.52 cM, were mapped. In the RS population, the total map length was 5545.98 cM and the average interval between loci was 15.41 cM. There were 486 markers assigned to 21 chromosomes with an average of 23 markers per chromosome. Chromosome 7D in the RS population was excluded from QTL mapping analysis since only one single marker was mapped to this chromosome. The linkage map for the RSH population consisted of 660 markers and spanned 5905.53 cM, with an average marker density of 10.89 cM. Additional information about the linkage maps is in Table 3.

QTL analysis

A total of 92 putative M-QTLs were identified across the 9 experiments (Table 4). Analyses of epistatic interactions among the M-QTLs, revealed, 3 E-QTLs (Table 5). Additionally, QTL by environment analyses detected a total of 67 intervals with significant additive main effects and/or additive by environment effects across multiple environments (Table 6 and Fig. 1). Of these, 49 intervals co-localized with M-QTLs whereas the remaining 18 intervals did not have a significant main effect in any of the 9 experiments (Table 6). Six of the 18 intervals had stable effects across different environments (Fig. 2). In the joint analysis, 57 QTLs were compared across the 3 mapping populations. All 57 QTLs were previously detected in the independent analysis, and 29 QTLs were in common between the joint and QTL by environment analyses.

The QTL analyses in single and multi-environments, epistatic interactions and genetic background are described in more detail in the following sections: joint analysis and independent analysis. The joint analysis section compares QTLs for common traits across the 3 mapping populations and the independent analysis section provides QTL information for individual mapping populations across environments.

Joint analysis

A total of 16 distinct M-QTLs for GYLD were detected across the 3 mapping populations (Table 7). Among these M-QTLs, 9 (56.25%) were identified in the RF population, while 3 (18.75%) and 4 (25%) were detected in the RS and RSH populations, respectively. These M-QTLs individually accounted for between 45.13% (RS population in Kerman 2012) and 2.60% (RF population in Kerman 2012) of GYLD variation. In the RF population, the positive alleles for 6 M-QTLs were derived from Roshan. In contrast, Roshan contributed only a single positive allele to RS and RSH M-QTLs. No common M-QTLs were identified across the 3 mapping populations. However, 3, 1 and 3 M-QTLs were detected across multiple environments in RF, RS and RSH, respectively via QTL by environment analysis. The other 9 M-QTLs were environment specific. Two M-QTLs (QGYLD.6A and QGYLD.3B) in RSH and a single M-QTL (QGYLD.1A) in RS displayed stable effects across

Table 2 Performance of recombinant inbred lines of Roshan × Falat (RF), Roshan × Sabalan (RF) and Roshan × Superhead#2 (RSH) for yield-related and morphological traits in Kerman-2013 (KR13), Kerman-2012 (KR12), Yazd-2011 (Y11)

Population	Trait	KR13				KR12				Y11			
		Max.	Min.	Mean	SD	Max.	Min.	Mean	SD	Max.	Min.	Mean	SD
RF	BYI (g/m^2)	795.00	144.50	376.11	120.35	1186.22	17.82	307.83	235.79	1485.00	510.00	979.32	187.49
	GYLD (g/m^2)	208.00	2.73	74.76	39.97	210.33	3.14	46.76	35.92	537.50	80.00	335.33	78.99
	HAI	0.38	0.01	0.19	0.07	0.32	0.03	0.17	0.06	0.49	0.13	0.34	0.05
	PHT (cm)	70.5	37.1	56.7	5.9	64.7	21.4	41.0	8.3	89.5	55.5	71.9	5.6
	SPL (cm)	11.1	4.8	7.6	1.1	15.7	4.2	8.7	2.3	10.6	5.3	7.7	0.7
	SPP	14.00	2.00	5.42	2.06	5.21	0.30	2.30	0.96	20.00	13.00	16.51	1.40
	SPW (g)	2.57	0.34	1.34	0.46	1.90	0.28	0.96	0.35	2.43	1.02	1.68	0.26
	TKW (g)	46.67	17.67	32.31	5.93	33.66	7.14	17.70	4.85	50.95	22.20	34.30	4.45
	WKP (g)	1.20	0.02	0.56	0.24	1.57	0.10	0.59	0.30	1.82	0.68	1.24	0.20
RS	BYI (g/m^2)	773.75	182.50	413.50	112.00	9738.75	27.02	2871.51	2367.64	1105.00	425.00	757.99	117.69
	GYLD (g/m^2)	247.62	12.98	95.77	53.05	337.33	3.20	94.32	72.90	420.00	137.50	283.09	52.93
	HAI	0.46	0.04	0.22	0.09	0.08	0.00	0.03	0.02	0.52	0.25	0.37	0.05
	PHT (cm)	71.7	43.0	60.2	5.0	67.3	15.4	43.8	8.4	92.0	59.0	75.2	6.1
	SPL (cm)	10.5	4.2	7.5	1.0	13.9	3.2	9.0	1.8	10.3	6.8	8.1	0.6
	SPW (g)	2.17	0.26	1.28	0.39	1.90	0.10	0.89	0.39	2.67	1.09	1.89	0.30
	TKW (g)	53.52	11.55	34.19	7.28	34.76	9.23	23.01	5.35	50.15	23.20	37.50	5.43
RSH	GYLD (g/m^2)	253.58	5.26	87.78	51.13	664.00	16.00	165.35	140.08	449.17	42.50	202.53	73.60
	PHT (cm)	72.0	39.0	56.6	6.0	94.5	32.3	69.3	12.3	108.1	60.1	85.5	9.8
	SPL (cm)	15.0	5.4	8.3	1.4	27.0	3.6	13.3	4.6	13.3	5.1	8.9	1.5
	TKW (g)	48.77	8.26	34.58	7.09	54.55	12.00	34.59	9.69	49.95	27.75	42.16	4.87

Min. minimum, *Max.* maximum, *SD* standard deviation, *PHT* plant height, *SPL* spike length, *SPW* spike weight, *WKP* weight of kernels in plant, *TKW* thousand kernel weight, *SPP* spike per plant, *GYLD* grain yield per plant, *BYI* biological yield per m^2, *HAI* harvest index, *RF* Roshan*Falat, *RS* Roshan*Sabalan, *RSH* Roshan*Superhead#2, *KR13* Kerman-2013, *KR12* Kerman-2012, *Y11* Yazd-2011

Table 3 Characteristics of the genetic maps employed in this study

Chr.[a]	Roshan *Falat					Roshan*Sabalan					Roshan*Superhead#2				
	N[b]	Length[c]	Max[d]	Min[e]	Ave[f]	N[b]	Length[c]	Max[d]	Min[e]	Ave[f]	N[b]	Length[c]	Max[d]	Min[e]	Ave[f]
1A	31	340.73	73.96	0.0	11.4	46	438.51	107.94	0.0	9.7	44	407.69	77.56	0.0	9.5
2A	32	345.49	49.75	0.0	11.1	10	160.22	41.73	0.0	17.8	29	396.97	59.65	0.0	14.2
3A	39	260.19	35.56	0.0	6.9	14	331.89	74.69	0.0	25.5	22	264.91	67.03	0.0	12.6
4A	32	181.22	63.72	0.0	5.9	35	338.88	62.24	0.0	10.0	36	181.63	57.29	0.0	5.2
5A	12	213.41	92.31	0.2	19.4	34	397.96	55.16	0.0	12.1	33	406.34	61.21	0.0	12.7
6A	38	249.03	74.35	0.0	6.7	5	191.25	119.47	0.2	47.8	28	383.84	60.84	0.0	14.2
7A	51	400.90	81.64	0.0	8.0	39	162.78	55.40	0.0	4.3	39	402.74	81.13	0.0	10.6
1B	85	293.29	27.47	0.0	3.5	29	288.12	74.04	0.0	10.3	26	370.13	93.74	0.0	14.8
2B	62	529.65	45.25	0.0	8.7	25	253.29	40.88	0.0	10.6	32	284.27	84.18	0.0	9.2
3B	125	684.72	69.14	0.0	5.5	52	364.42	53.08	0.0	7.2	44	462.86	53.73	0.0	10.8
4B	25	277.13	59.60	0.0	11.6	13	156.82	51.72	0.0	13.1	12	276.45	78.07	0.0	25.1
5B	30	383.95	68.07	0.0	13.2	27	164.99	43.15	0.0	6.4	8	70.54	69.31	0.0	10.1
6B	53	478.66	42.62	0.0	9.2	16	430.87	100.64	0.0	28.7	15	134.43	70.53	0.0	9.6
7B	44	343.32	43.77	0.0	8.0	2	0.21	0.21	0.2	0.2	130	164.14	39.61	0.0	1.3
1D	47	133.08	18.28	0.0	2.9	15	192.12	83.08	0.0	13.7	25	168.26	30.48	0.0	7.0
2D	30	341.75	142.00	0.0	11.8	12	189.50	107.94	0.0	17.2	33	371.74	84.47	0.0	11.6
3D	23	226.56	75.18	0.0	10.3	31	332.24	100.19	0.0	11.1	18	227.08	54.34	0.0	13.4
4D	3	15.78	15.24	0.5	7.9	10	345.45	107.03	0.2	38.4	10	95.48	30.33	2.7	10.6
5D	8	80.04	27.80	0.3	11.4	41	419.46	64.40	0.0	10.5	40	356.25	52.27	0.0	9.1
6D	10	226.94	78.56	0.2	25.2	29	387.00	115.13	0.0	13.8	34	477.05	59.95	0.0	14.5
7D	30	90.04	16.97	0.0	3.1	1	–	–	–	–	2	2.73	2.73	2.7	2.7
Total	810	6095.88	142.00	0.0	7.7	486	5545.98	119.47	0.0	11.9	660	5905.53	93.74	0.0	9.2
A	235	1990.97	92.31	0.0	7.3	183	2021.49	119.47	0.0	11.3	231	2444.12	81.13	0.0	11.3
B	424	2990.72	69.14	0.0	7.2	164	1658.72	100.64	0.0	10.6	267	1762.82	93.74	0.0	9.8
D	151	1114.19	142.00	0.0	7.7	139	1865.77	115.13	0.0	14.1	162	1698.59	84.47	0.0	11.0

[a]Chromosome

[b]Number of DArT markers

[c]Length of map

[d]Maximum interval

[e]Minimum interval

[f]Average interval

environments (Fig. 2). No epistatic interactions were identified for M-QTLs associated with GYLD.

For PHT, 11 and 7 M-QTLs were discovered in the RF and RSH populations, respectively, whereas only a single M-QTL was detected in the RS population (Table 7). Two of the M-QTLs (QPHT.6D-2, QPHT.7A-3) in RSH explained greater than 20% of phenotypic variance (i.e., major QTLs). In contrast, none of the 12 M-QTLs in the RS and RF populations had a major effect. Roshan alleles increased PHT by an average of 2.78 cm (ranging from 2.34 to 3.10 cm) in RSH, but only by 0.91 and 1.83 cm in RS and RF, respectively. A comparison of the 9 experiments revealed that QPHT.7A-2 and QPHT.7A-3 are probably the same QTL across two different genetic backgrounds (RF and RSH) in the same environment (Kerman-2013). In addition, 11 M-QTLs have significant QTL by environment effects. Conversely, the

Table 4 Independent analysis, genomic regions associated with yield-related and morphological traits in different genetic backgrounds and environments

Trait	QTL	Pop[a]	ENV[b]	Chr.	Pos.	Marker interval	LOD	PVE[c] (%)	Add[d]	+Allele[e]
BYI	QBYI.2A-1	RF	Kr13	2A	90	wPt-7721–wPt-7187	3.3039	3.4964	0.5605	Roshan
	QBYI.2A-2	RF	Kr12	2A	95	wPt-7187–wPt-115	3.2618	3.4926	1.2366	Roshan
	QBYI.7A	RF	Y11	7A	225	wPt-4960–wPt-3523	4.7094	7.0759	0.8213	Roshan
	QBYI.7B-1	RF	Kr13	7B	155	wPt-6484–wPt-6657	5.9391	7.4994	0.8059	Roshan
	QBYI.7B-2	RF	Kr13	7B	330	wPt-4230–wPt-8283	3.5874	3.7623	0.5690	Roshan
	QBYI.4D	RS	Kr13	4D	345	wPt-8794–wPt-733910	3.0688	3.8256	− 0.5090	Sabalan
GYLD	QGYLD.1B	RF	Kr12	1B	180	wPt-320–wPt-6434	3.5866	3.4222	0.7028	Roshan
	QGYLD.2A-1	RF	Kr12	2A	95	wPt-7187–wPt-115	3.0578	2.8703	0.4360	Roshan
	QGYLD.2A-2	RF	Y11	2A	320	wPt-6687–wPt-729945	3.3546	7.9449	− 0.6110	Falat
	QGYLD.2B	RF	Kr13	2B	300	wPt-6932–wPt-4301	3.4948	4.2513	0.4721	Roshan
	QGYLD.3D	RF	Kr13	3D	50	wPt-7241–wPt-730935	3.1998	3.6667	− 0.4490	Falat
	QGYLD.4D-1	RF	Kr12	4D	0	wPt-3058–wPt-672143	3.0529	2.6050	0.4492	Roshan
	QGYLD.6A-2	RF	Kr12	6A	160	wPt-228–wPt-741630	3.6348	4.5674	− 0.6482	Falat
	QGYLD.7A	RF	Y11	7A	225	wPt-4960–wPt-3523	3.9589	5.2413	0.5157	Roshan
	QGYLD.7B	RF	Kr13	7B	155	wPt-6484–wPt-6657	4.6688	5.4045	0.5331	Roshan
	QGYLD.6A-1	RS	Kr13	6A	20	wPt-9589–wPt-653	3.9476	15.1472	− 1.0562	Sabalan
	QGYLD.1A	RS	Y11	1A	110	wPt-664968–wPt-5316	3.4660	4.7872	0.3450	Roshan
	QGYLD.6B	RS	Kr12	6B	95	wPt-494–wPt-741686	3.0253	45.1356	2.4571	Roshan
	QGYLD.6A-3	RSH	Kr13	6A	380	wPt-5037–wPt-669672	3.7796	5.3191	0.6092	Roshan
	QGYLD.1D	RSH	Y11	1D	0	wPt-731338–wPt-667083	3.3204	5.4482	− 0.5941	Superhead#2
	QGYLD.3B	RSH	Kr13	3B	160	wPt-731378–wPt-2559	3.8335	6.5998	− 0.6797	Superhead#2
	QGYLD.4D-2	RSH	Kr13	4D	20	wPt-7769–wPt-665622	3.1595	4.4888	− 0.5595	Superhead#2
HAI	QHAI.4D-1	RF	Y11	4D	5	wPt-3058–wPt-4572	3.0969	5.6897	0.0124	Roshan
	QHAI.5A-2	RF	Kr12	5A	185	wPt-4249–wPt-3334	5.8609	19.6774	− 0.0274	Falat
	QHAI.2A	RF	Kr13	2A	120	wPt-664128–wPt-1114	3.3323	3.3960	0.0140	Roshan
	QHAI.2B	RF	Kr12	2B	290	wPt-3561–wPt-4997	4.6507	5.6591	0.0141	Roshan
	QHAI.3B-1	RF	Kr12	3B	360	wPt-4220–wPt-669517	5.3456	8.2628	− 0.0178	Falat
	QHAI.3B-2	RF	Kr13	3B	480	wPt-8781–wPt-10948	3.7460	3.8287	0.0132	Roshan
	QHAI.6D-1	RF	Kr13	6D	95	wPt-729831–wPt-5331	3.1923	3.2437	− 0.0122	Falat
	QHAI.4D-2	RS	Y11	4D	275	wPt-3563–wPt-8794	3.1755	5.9101	0.0110	Roshan
	QHAI.5A-1	RS	Kr12	5A	55	tPt-8942–wPt-1505	3.5624	20.0412	− 0.0100	Sabalan
	QHAI.1B	RS	Kr12	1B	55	wPt-734314–wPt-7259	5.4342	41.9097	− 0.0143	Sabalan
	QHAI.5B	RS	Kr13	5B	130	wPt-731592–wPt-7809	3.7279	18.2084	− 0.0543	Sabalan
	QHAI.6A	RS	Kr13	6A	15	wPt-9589–wPt-653	3.8039	13.5752	− 0.0338	Sabalan
	QHAI.6D-2	RS	Kr12	6D	130	wPt-3873–wPt-8007	4.2693	9.0634	0.0089	Roshan

Table 4 continued

Trait	QTL	Pop[a]	ENV[b]	Chr.	Pos.	Marker interval	LOD	PVE[c] (%)	Add[d]	+Allele[e]
PHT	QPHT.7A-2	RF	Kr13	7A	315	wPt-3992–wPt-3393	4.0100	6.1260	− 1.4368	Falat
	QPHT.1B	RF	Y11	1B	0	wPt-1070–wPt-734314	3.1013	3.6665	− 1.1017	Falat
	QPHT.2A	RF	Y11	2A	200	wPt-9277–wPt-1142	3.0361	5.1977	1.2699	Roshan
	QPHT.3B	RF	Kr12	3B	365	wPt-669517–wPt-446	4.3793	5.9044	− 2.1957	Falat
	QPHT.3D	RF	Kr12	3D	30	wPt-7241–wPt-730935	3.6870	17.3622	3.4077	Roshan
	QPHT.4B-3	RF	Kr12	4B	260	wPt-671760–wPt-5730	4.1320	5.1507	− 1.8533	Falat
	QPHT.6B-2	RF	Kr13	6B	190	wPt-669672–wPt-8554	4.2728	6.0601	− 1.4661	Falat
	QPHT.6B-3	RF	Y11	6B	355	wPt-4858–wPt-745128	4.6020	6.3632	1.3875	Roshan
	QPHT.6B-4	RF	Y11	6B	450	wPt-406–wPt-9952	3.5072	4.7324	1.2087	Roshan
	QPHT.7A-1	RF	Kr13	7A	45	wPt-2260–wPt-741686	3.2447	4.7206	1.2984	Roshan
	QPHT.7B	RF	Kr13	7B	155	wPt-6484–wPt-6657	13.7044	17.9018	2.4478	Roshan
	QPHT.6D-1	RS	Kr13	6D	315	wPt-7251–wPt-465	3.0662	3.6632	0.9148	Roshan
	QPHT.7A-3	RSH	Kr13	7A	340	wPt-7925–wPt-8920	11.9740	21.5644	3.1027	Roshan
	QPHT.1D	RSH	Y11	1D	165	wPt-3738–wPt-665480	3.8317	8.3126	2.7448	Roshan
	QPHT.4B-1	RSH	Y11	4B	190	wPt-5390–wPt-4931	5.0280	9.7101	2.9625	Roshan
	QPHT.4B-2	RSH	Kr13	4B	215	wPt-872–wPt-391	8.3622	16.1830	2.3401	Roshan
	QPHT.6A	RSH	Y11	6A	360	wPt-3778–wPt-3733	3.8608	7.3232	− 2.5705	Superhead#2
	QPHT.6B-1	RSH	Kr13	6B	20	wPt-7394–wPt-8166	3.6290	5.0224	− 1.3076	Superhead#2
	QPHT.6D-2	RSH	Kr12	6D	415	wPt-7108–wPt-3226	3.4058	22.5462	− 9.6882	Superhead#2
SPL	QSPL.3B	RF	Kr12	3B	520	wPt-6802–wPt-5769	3.5016	3.3290	0.0729	Roshan
	QSPL.3D	RF	Kr12	3D	40	wPt-7241–wPt-730935	3.2706	5.7567	0.0934	Roshan
	QSPL.4B	RF	Kr12	4B	260	wPt-671760–wPt-5730	37.1734	39.0704	− 0.2410	Falat
	QSPL.6B	RF	Kr13	6B	175	wPt-9124–wPt-1730	5.0646	6.2210	0.0481	Roshan
	QSPL.7A	RF	Kr13	7A	305	wPt-4515–wPt-4744	3.2719	3.9020	− 0.0371	Falat
	QSPL.7B	RF	Kr13	7B	275	wPt-2305–wPt-3833	3.0644	3.7786	− 0.0373	Falat
	QSPL.1B	RS	Y11	1B	55	wPt-734314–wPt-7259	3.0829	24.5325	− 0.4226	Sabalan
	QSPL.4A	RS	Y11	4A	310	wPt-672143–wPt-667538	3.2591	15.8203	0.2188	Roshan
	QSPL.5A	RS	Kr12	5A	65	tPt-8942–wPt-1505	3.9247	12.7455	0.7635	Roshan
	QSPL.3A	RSH	Kr12	3A	60	wPt-3389–wPt-664504	6.0098	42.9634	0.5083	Roshan
SPP	QSPP.1A	RF	Kr13	1A	40	wPt-9429–wPt-733007	3.7898	4.2002	0.4119	Roshan
	QSPP.5A	RF	Kr12	5A	180	wPt-4249–wPt-3334	3.4454	5.3903	0.2638	Roshan
SPW	QSPW.1B	RF	Kr12	1B	200	wPt-8177–wPt-1251	3.7433	6.5361	− 0.1098	Falat
	QSPW.2A	RF	Kr13	2A	90	wPt-7721–wPt-7187	5.8987	9.1622	0.1385	Roshan
	QSPW.2B	RF	Kr13	2B	300	wPt-6932–wPt-4301	3.4591	4.7276	0.0975	Roshan
	QSPW.3B	RF	Kr12	3B	365	wPt-669517–wPt-446	3.3072	4.6260	− 0.0821	Falat
	QSPW.7D	RF	Kr13	7D	0	wPt-669587–wPt-5489	3.0603	3.8766	− 0.0889	Falat
	QSPW.4B	RS	Kr12	4B	0	wPt-1101–wPt-2525	3.2512	3.6471	0.0735	Roshan
	QSPW.5D	RS	Kr13	5D	95	wPt-8336–wPt-664937	3.1979	28.7125	− 0.2114	Sabalan
	QSPW.7A	RS	Kr13	7A	50	wPt-665471–wPt-664252	3.3481	4.2773	0.0776	Roshan

Table 4 continued

Trait	QTL	Pop[a]	ENV[b]	Chr.	Pos.	Marker interval	LOD	PVE[c] (%)	Add[d]	+Allele[e]
TKW	QTKW.3B-1	RF	Kr12	3B	365	wPt-669517–wPt-446	5.5150	8.1435	− 1.4917	Falat
	QTKW.1B-1	RF	Kr13	1B	140	wPt-6012–wPt-3451	3.1680	4.3216	1.2318	Roshan
	QTKW.1B-2	RF	Y11	1B	270	wPt-1248–wPt-9857	3.2682	5.1372	− 1.5757	Falat
	QTKW.2A	RF	Kr13	2A	95	wPt-7187–wPt-115	3.1329	4.3304	1.2225	Roshan
	QTKW.3A-2	RF	Kr12	3A	220	wPt-9761–wPt-6422	3.0145	3.9299	− 0.9558	Falat
	QTKW.5D	RF	Kr12	5D	40	wPt-5505–wPt-2256	4.6804	6.5939	1.4917	Roshan
	QTKW.3A-1	RS	Kr13	3A	75	wPt-8699–wPt-733571	3.6193	5.7961	− 1.6934	Sabalan
	QTKW.3B-2	RSH	Kr12	3B	365	wPt-3094–wPt-7212	3.7615	7.8024	− 1.9404	Superhead#2
	QTKW.1A	RSH	Y11	1A	95	wPt-668205–wPt-664666	5.9067	14.8009	1.7732	Roshan
	QTKW.5B	RSH	Kr13	5B	0	wPt-1400–wPt-663848	14.4912	33.0543	4.2248	Roshan
	QTKW.6A	RSH	Kr12	6A	310	wPt-6282–wPt-7954	3.9683	7.0318	− 1.8162	Superhead#2
	QTKW.7A	RSH	Kr13	7A	335	wPt-664218–wPt-7925	3.2871	4.4880	1.5285	Roshan
WKP	QWKP.1B	RF	Kr13	1B	230	tPt-7214–tPt-5515	3.5168	4.8742	− 0.0707	Falat
	QWKP.1D	RF	Y11	1D	20	wPt-6461–wPt-3790	3.7528	4.0242	0.0418	Roshan
	QWKP.2B	RF	Kr13	2B	305	wPt-4301–wPt-8349	3.4493	3.5135	0.0432	Roshan
	QWKP.3B	RF	Kr12	3B	365	wPt-669517–wPt-446	5.6965	8.9129	− 0.0981	Falat
	QWKP.4A-1	RF	Kr13	4A	130	wPt-1961–wPt-8091	3.3822	5.2109	− 0.0548	Falat
	QWKP.4A-2	RF	Kr13	4A	180	wPt-5172–wPt-6900	4.0953	5.3082	0.0539	Roshan

Min. minimum, *Max.* maximum, *SD* standard deviation, *PHT* plant height, *SPL* spike length, *SPW* spike weight, *WKP* weight of kernels in plant, *TKW* thousand kernel weight, *SPP* spike per plant, *GYLD* grain yield per m^2, *BYI* biological yield per m^2, *HAI* harvest index, *RF* Roshan*Falat, *RS* Roshan*Sabalan, *RSH* Roshan*Superhead#2, *KR13* Kerman-2013, *KR12* Kerman-2012, *Y11* Yazd-2011

[a]Mapping population for detected QTL

[b]The environment of detected QTL

[c]Phenotypic variation explained

[d]Additive effect of detected QTL

[e]Source of positive allele

other 8 M-QTLs had environment specific effects. Notably, strong evidence of stability across environments was found for 6 M-QTLs via biplot analysis (Fig. 2). No significant epistatic interactions were detected for M-QTLs underlying PHT.

Ten M-QTLs were discovered to be associated with SPL (Table 7). Of these, the majority (6) were identified in the RF population, whereas 3 M-QTLs were identified in RS and 1 in RSH. Of the 10 M-QTLs, one in each population had a major effect. Roshan contributed positive alleles to 3 M-QTLs in the RF population, 2 M-QTLs in the RS population and one in the RSH population. No common M-QTLs were found across the three mapping populations, although 4 M-QTLs had exhibited significant QTL by environment effects. Only one M-QTL (QSPL.3A) demonstrated environmental stability (Fig. 2). No

epistatic interactions were observed among M-QTLs associated with SPL.

For TKW, 6, 5 and 1 M-QTLs were identified in the RF, RSH and RS populations, respectively (Table 7). Of these, only a single M-QTL (QTKW.5B) had a major effect in the RSH population at Kerman-2013. Analysis of epistatic interactions revealed a single significant interaction between QTKW.3B-2 and a locus on chromosome 3D (Table 5). QTL by environment analysis revealed that environment had a significant effect on 4 M-QTLs in RSH, 3 in the RF, but none in RS. Only two M-QTLs (QTKW.7A-2 and QTKW.5B), both in the RSH population, were found to be environmentally stable (Fig. 2).

Table 5 QTL epistatic effects associated with yield-related and morphological traits in different genetic backgrounds and environments

QTL	Chr1	Marker interval 1	Chr2	Marker interval 2	LOD	PVE[a] (%)	Add[b]1	Add2	Addbyadd
QSPP.5A	5A	wPt-4249–wPt-3334	5B	wPt-3289–wPt-6498	5.5488	37.1434	− 0.8571	− 1.0352	1.1280
QSPP.5A	5A	wPt-4249–wPt-3334	3B	wPt-734202–wPt-7341	5.7492	25.4451	− 0.9204	1.5336	− 1.8572
QTKW.3B-2	3B	wPt-3094–wPt-7212	3D	wPt-4569–wPt-7705	6.3629	36.2533	− 6.3688	− 0.1637	− 5.6741

[a] Phenotypic variation explained

[b] Additive effect of QTL

Independent analysis

RF population

Fifty-seven M-QTLs were found to be associated with 9 traits in the RF population (Supplementary Figure 4). The majority of M-QTLs (26) were identified in the Kerman-2013 environment. In addition, 21 and 10 M-QTLs were discovered in Kerman-2012 and Yazd-2011, respectively (Supplementary Figure 5). The largest number of M-QTLs in this population were associated with PHT (11) followed by GYLD (9), HAI (7), TKW (6), SPL (6), WKP (6), SPW (5), BYI (5) and SPP (2). A single QTL (QSPL.4B) was detected that explained > 20% of the spike length variation. Epistatic interaction results indicated that an M-QTL associated with SPP on chromosome 5 (QSPP.5A) had epistatic interactions (Table 5). QTL by environment analysis detected 34 intervals, which co-localized with M-QTLs in RF. Of these, QPHT.6B-2, QBYI.7A, QBYI.7B-1 were found to be stable across environments (Fig. 2).

RS population

Of 18 M-QTLs detected for 7 traits in the RS population, 8 M-QTLs were identified in the Kerman-2013 environment, while 6 and 4 M-QTLs were discovered in Kerman-2012 and Yazd-2011, respectively (Supplementary Figure 5). QGYLD.6B and QHAI.1B were recognized as major QTLs. Four M-QTLs had significant effects in the QTL by environment analysis (Table 6). Only QGYLD.1A was found to be stable across environments as shown by the biplot analysis (Fig. 2). No evidence of significant epistatic interactions was found among M-QTLs in RS.

RSH population

Seventeen M-QTLs were found to be associated with 4 traits in the RSH population (Supplementary Figure 6). The largest number of M-QTLs (7) were identified for PHT, while the fewest M-QTLs (1) were associated with SPL. Five and 4 M-QTLs were found to be associated with TKW and GYLD, respectively. QSPL.3A, QTKW.5B, QPHT.6D-2 and QPHT.7A-3 represent major M-QTLs. Significant QTL by environment effects were found for 11 M-QTLs (Table 6).

Table 6 Main additive and additive by environment effect of most significant QTLs associated yield-related and morphological traits across different genetic backgrounds and environments

Trait	QTL	Chr.	Pos.	Marker interval	LOD	PVE[a]	Add[b]	A*KR13[c]	A*KR12[d]	A*Y11[e]	M-QTL[F]
BYI	QBYI.2A	2A	90	wPt-7721–wPt-7187	3.7023	1.9162	0.3661	− 0.0057	0.6171	− 0.6114	QBYI.2A-1
	QBYI.4D	4D	345	wPt-8794–wPt-733910	3.3957	0.6107	− 0.7130	0.2185	− 0.9357	0.7172	QBYI.4D
	QBYI.7A	7A	225	wPt-4960–wPt-3523	3.3832	1.0142	1.1077	0.0649	− 0.5836	0.5188	QBYI.7A
	QBYI.7B-2	7B	330	wPt-4230–wPt-8283	3.1147	0.6529	0.1594	0.3605	0.0512	− 0.4118	QBYI.7B-2
	QBYI.7B-1	7B	155	wPt-6484–wPt-6657	4.8845	1.2975	0.5004	0.0606	− 0.0381	− 0.0225	QBYI.7B-1
GYLD	QGYLD.1A	1A	110	wPt-664968–wPt-5316	3.3681	0.6790	0.3171	− 0.0990	0.0286	0.0704	QGYLD.1A
	QGYLD.1B	1B	195	wPt-2786–wPt-4721	3.4802	1.7892	− 0.1041	− 0.3851	− 0.2124	0.5976	
	QGYLD.1D	1D	0	wPt-731338–wPt-667083	3.5092	1.3156	− 0.1239	0.4675	− 0.0781	− 0.3893	QGYLD.1D
	QGYLD.2A	2A	90	wPt-7721–wPt-7187	3.8851	1.6180	0.1690	0.1708	0.1803	− 0.3511	
	QGYLD.2B	2B	300	wPt-6932–wPt-4301	4.1887	1.9550	0.2723	0.1929	0.0386	− 0.2315	QGYLD.2B
	QGYLD.3B	3B	160	wPt-731378–wPt-2559	3.2977	2.1916	− 1.4406	− 0.1180	− 0.1672	0.2852	QGYLD.3B
	QGYLD.4D	4D	345	wPt-8794–wPt-733910	3.2075	2.0337	− 0.3349	− 0.1907	− 0.0865	0.2772	
	QGYLD.6A	6A	380	wPt-5037–wPt-669672	3.5002	1.3246	1.0058	0.3094	− 0.1778	− 0.1316	QGYLD.6A-3
	QGYLD.6D	6D	245	wPt-664948–wPt-6217	3.6421	2.0769	− 0.1406	− 0.3770	− 0.2635	0.6406	
	QGYLD.7A	7A	225	wPt-4960–wPt-3523	3.8222	1.6260	0.0528	− 0.0080	− 0.3657	0.3736	QGYLD.7A
	QGYLD.7B	7B	155	wPt-6484–wPt-6657	3.2376	1.4154	0.2281	0.1987	− 0.1810	− 0.0178	QGYLD.7B
HAI	QHAI.2A	2A	90	wPt-7721–wPt-7187	3.1105	1.4455	0.0006	0.0097	− 0.0065	− 0.0032	
	QHAI.2B	2B	295	wPt-4997–wPt-6932	4.8723	2.2758	0.0083	0.0025	0.0012	− 0.0037	
	QHAI.3B-1	3B	365	wPt-669517–wPt-446	6.5580	2.6316	− 0.0054	0.0069	− 0.0122	0.0053	
	QHAI.3B-2	3B	480	wPt-8781–wPt-10948	3.0686	1.3094	0.0039	0.0074	− 0.0031	− 0.0043	QHAI.3B-2
	QHAI.4D	4D	0	wPt-3058–wPt-672143	3.0043	0.8979	0.0032	− 0.0045	− 0.0026	0.0072	
	QHAI.6D	6D	95	wPt-729831–wPt-5331	3.4601	1.3860	− 0.0022	− 0.0089	0.0055	0.0034	QHAI.6D-1

Table 6 continued

Trait	QTL	Chr.	Pos.	Marker interval	LOD	PVE[a]	Add[b]	A*KR13[c]	A*KR12[d]	A*Y11[e]	M-QTL[F]
PHT	QPHT.1D	1D	165	wPt-3738–wPt-665480	3.9063	1.8617	0.9329	− 0.4496	− 0.7473	1.1969	QPHT.1D
	QPHT.3B	3B	365	wPt-669517–wPt-446	4.1162	2.2987	− 0.7250	0.7015	− 1.1724	0.4709	QPHT.3B
	QPHT.4B-2	4B	260	wPt-671760–wPt-5730	4.7081	2.7172	− 0.4722	0.8581	-1.3681	0.5101	QPHT.4B-3
	QPHT.4B-1	4B	195	wPt-872–wPt-391	3.2114	1.6655	1.1381	− 0.1734	− 0.3341	0.5075	QPHT.4B-2
	QPHT.6A	6A	355	wPt-664142–wPt-3778	3.7162	2.0206	-1.3001	0.2405	− 0.2509	0.0103	
	QPHT.6B-3	6B	450	wPt-406–wPt-9952	3.2527	0.6568	0.3236	− 0.3513	− 0.2563	0.6076	QPHT.6B-4
	QPHT.6B-2	6B	355	wPt-4858–wPt-745128	3.5841	1.0426	0.5554	− 0.1572	− 0.3664	0.5236	QPHT.6B-3
	QPHT.6B-1	6B	190	wPt-669672–wPt-8554	3.4437	1.1552	− 0.4909	− 0.7178	0.1222	0.5956	QPHT.6B-2
	QPHT.7A-2	7A	45	wPt-2260–wPt-741686	3.2451	0.6869	0.2848	0.6518	− 0.1272	− 0.5246	QPHT.7A-1
	QPHT.7A-3	7A	315	wPt-3992–wPt-3393	3.8883	0.9107	− 0.4358	− 0.5514	− 0.0196	0.5711	QPHT.7A-2
	QPHT.7A-4	7A	340	wPt-7925–wPt-8920	5.6119	2.1817	0.8172	1.3470	-1.8312	0.4842	QPHT.7A-3
	QPHT.7A-1	7A	30	wPt-9342–wPt-504	3.4208	1.1080	− 0.9867	− 0.0914	0.1628	− 0.0714	
	QPHT.7B-3	7B	315	wPt-4230–wPt-8283	3.1205	0.7902	0.5951	0.0815	0.0604	− 0.1419	
	QPHT.7B-1	7B	95	wPt-4300–wPt-7108	3.6023	1.0474	− 0.6340	− 0.1951	− 0.2762	0.4714	
	QPHT.7B-2	7B	155	wPt-6484–wPt-6657	4.7046	1.9508	0.1575	1.0692	-1.1531	0.0839	QPHT.7B
SPL	QSPL.3A	3A	0	wPt-3389–wPt-664504	3.2165	3.9128	1.9409	− 0.0508	0.0891	− 0.0382	QSPL.3A
	QSPL.3B	3B	515	wPt-4364–wPt-6802	4.5658	2.0632	0.0270	− 0.0052	0.0351	− 0.0299	
	QSPL.3D	3D	50	wPt-7241–wPt-730935	3.2154	1.8291	0.0232	− 0.0199	0.0385	− 0.0186	QSPL.3D
	QSPL.4B	4B	260	wPt-671760–wPt-5730	36.4194	26.5693	− 0.0812	0.0683	− 0.1485	0.0802	QSPL.4B
	QSPL.6B-2	6B	210	wPt-741804–wPt-7662	4.9108	0.9111	− 0.0145	− 0.0355	0.0156	0.0198	
	QSPL.6B-1	6B	175	wPt-9124–wPt-1730	3.6102	0.6263	0.0182	0.0136	− 0.0021	− 0.0115	QSPL.6B
	QSPL.7B	7A	275	wPt-2305–wPt-3833	3.9334	0.9647	0.0038	− 0.0314	0.0314	0.0000	
SPP	QSPP.1A	1A	40	wPt-9429–wPt-733007	3.8708	2.2374	0.1244	0.2640	− 0.0881	− 0.1759	QSPP.1A
	QSPP.5A	5A	180	wPt-4249–wPt-3334	3.4739	0.4747	0.0974	− 0.0080	0.0978	− 0.0898	QSPP.5A
SPW	QSPW.2A	2A	90	wPt-7721–wPt-7187	7.5464	4.0649	0.0567	0.0605	− 0.0076	− 0.0529	QSPW.2A
	QSPW.2B	2B	300	wPt-6932–wPt-4301	4.2311	2.4802	0.0440	0.0476	− 0.0115	− 0.0361	QSPW.2B
	QSPW.3B	3B	365	wPt-669517–wPt-446	5.5646	2.0824	− 0.0240	0.0369	− 0.0730	0.0361	QSPW.3B
	QSPW.4B	4B	0	wPt-11101–wPt-2525	3.7140	1.6711	0.0092	− 0.0173	0.0618	− 0.0445	QSPW.4B
	QSPW.7A	7A	50	wPt-665471–wPt-664252	3.4308	1.5782	0.0250	0.0515	− 0.0303	− 0.0213	QSPW.7A
	QSPW.7D	7D	0	wPt-669587–wPt-5489	3.1150	2.0524	− 0.0335	− 0.0554	0.0270	0.0284	QSPW.7D

Table 6 continued

Trait	QTL	Chr.	Pos.	Marker interval	LOD	PVE[a]	Add[b]	A*KR13[c]	A*KR12[d]	A*Y11[e]	M-QTL[F]
TKW	QTKW.1A	1A	95	wPt-668205–wPt-664666	3.0471	0.7860	0.2257	− 0.4111	− 0.2867	0.6978	QTKW.1A
	QTKW.1B	1B	270	wPt-1248–wPt-9857	3.0795	1.0498	− 0.4412	0.5166	0.4464	− 0.9631	QTKW.1B-2
	QTKW.2A	2A	95	wPt-7187–wPt-115	3.8486	2.0621	0.1652	0.9964	− 0.6650	− 0.3314	QTKW.2A
	QTKW.3A	3A	70	wPt-1119–wPt-8699	3.7811	1.9868	− 0.6918	− 0.6236	0.4556	0.1680	
	QTKW.3B	3B	365	wPt-669517–wPt-446	4.3754	1.9459	− 0.6292	− 0.1383	− 0.4427	0.5809	QTKW.3B-1
	QTKW.5B	5B	0	wPt-1400–wPt-663848	3.7864	2.9028	1.0335	0.6782	− 0.4156	− 0.2626	QTKW.5B
	QTKW.6A	6A	310	wPt-6282–wPt-7954	3.7591	2.3953	− 0.6938	0.2411	− 0.8950	0.6538	QTKW.6A
	QTKW.6D	6D	105	wPt-665920–wPt-8	3.3892	2.7512	1.1891	0.6315	0.6919	-1.3234	
	QTKW.7A-2	7A	335	wPt-664218–wPt-7925	3.7414	2.9324	0.6474	1.1024	-1.1525	0.0502	QTKW.7A
	QTKW.7A-1	7A	45	wPt-667894–wPt-733729	3.2135	1.4429	0.5294	0.4601	− 0.6413	0.1812	
WKP	QWKP.1B	1B	230	tPt-7214–tPt-5515	3.8448	1.4170	0.0039	− 0.0413	0.0557	− 0.0144	QWKP.1B
	QWKP.1D	1D	20	wPt-6461–wPt-3790	3.5119	1.1026	0.0109	− 0.0345	0.0204	0.0141	QWKP.1D
	QWKP.2B	2B	305	wPt-4301–wPt-8349	3.9659	1.8234	0.0282	0.0131	0.0117	− 0.0248	QWKP.2B
	QWKP.3B	3B	365	wPt-669517–wPt-446	4.2151	2.4704	− 0.0187	0.0261	− 0.0544	0.0283	QWKP.3B
	QWKP.4A	4A	180	wPt-5172–wPt-6900	3.1529	0.8732	0.0048	0.0324	− 0.0153	− 0.0171	QWKP.4A-2

Min. minimum, *Max.* maximum, *SD* standard deviation, *PHT* plant height, *SPL* spike length, *SPW* spike weight, *WKP* weight of kernels in plant, *TKW* thousand kernel weight, *SPP* spike per plant, *GYLD* grain yield per m², *BYI* biological yield per m², *HAI* harvest index, *RF* Roshan*Falat, *RS* Roshan*Sabalan, *RSH* Roshan*Superhead#2, *KR13* Kerman-2013, *KR12* Kerman-2012, *Y11* Yazd-2011

[a] Phenotypic variation explained

[b] Additive effect of detected QTL

[c] Additive by Environment (Kerman-2013) effect

[d] Additive by Environment (Kerman-2012) effect

[e] Additive by Environment (Yazd-2011) effect
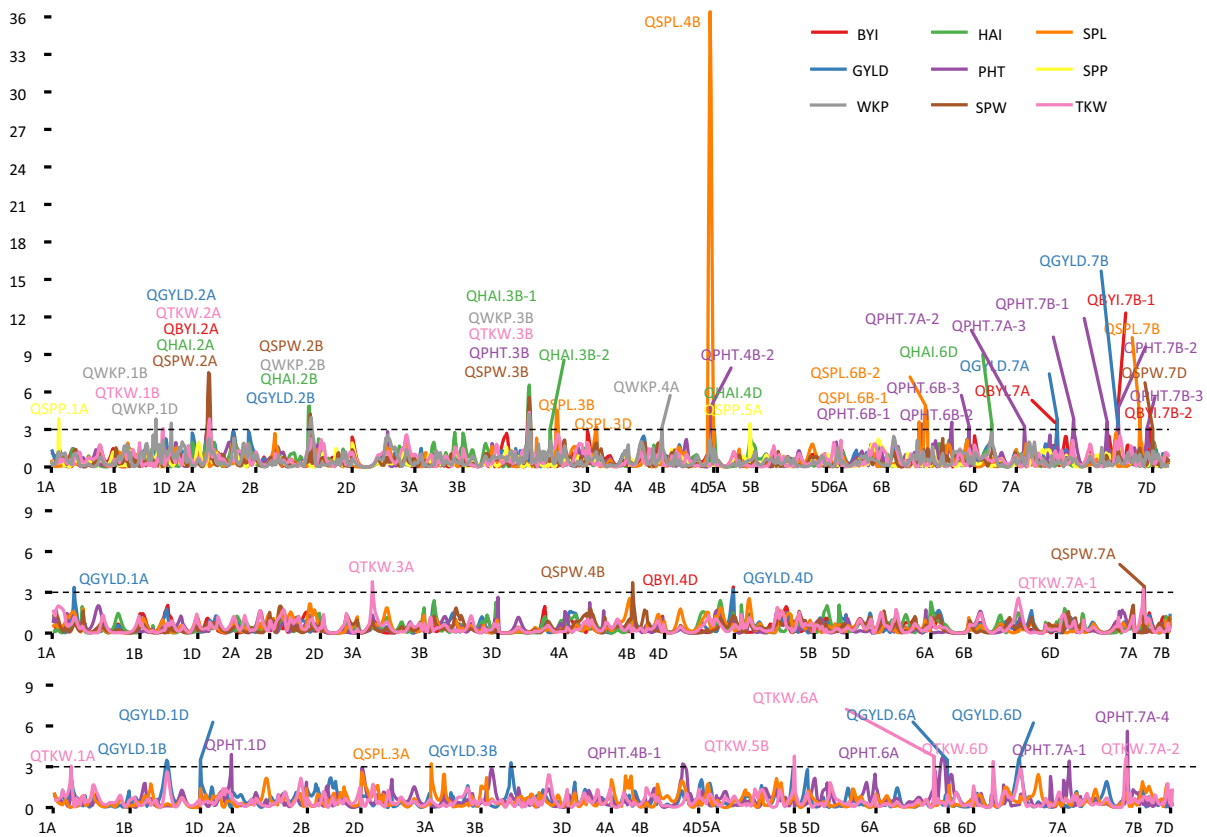
[f] Co-localized M-QTLs

Fig. 1 LOD profile of plant height (PHT), spike length (SPL), spike weight (SPW), weight of kernels in plant (WKP), thousand kernel weight (TKW), spikes per plant (SPP), grain yield per m² (GYLD), biological yield per m² (BYI), harvest index (HAI) in different genetic backgrounds; Roshan*Falat (RF), Roshan*Sabalan (RS), Roshan*Superhead#2 (RSH) across environments

Of these, QTKW.7A-2, QTKW.5B, QSPL.3A, QPHT.4B-1, QPHT.1D, QGYLD.6A and QGYLD.3B had stable effects across environments (Fig. 2). Significant epistatic interactions were only detected for QTKW.3B-2 (Table 5).

Discussion

The majority of wheat breeders have focused on enhancing drought tolerance, with relatively less effort directed towards salt tolerance (Munns et al. 2006). However, given the fairly large fraction of agricultural land affected by salt (Flowers and Yeo 1995), and the extent of yield losses when growing wheat on such land (Sardouie-Nasab et al. 2013), a greater focus on the development of salt tolerant wheat varieties is increasingly critical. Fortunately, significant variation for salt tolerance can be found in the cultivar gene pool, so the development of such cultivars should be straightforward, although success (and speed) will depend on the genetic architecture and stability of traits associated with salt tolerance.

Genetic background

Recent advances in genomics and computational biology offer a means for dissecting the genetic architecture of complex traits such as salt tolerance. Furthermore, utilizing new genomic tools in marker-aided breeding programs can accelerate identification and selection of desired genes compared to classical breeding (Hussain 2015; Saade et al. 2016; Budak et al. 2004; Jahani et al. 2014; Castillo et al. 2008). However, the successful implementation of MAS requires that GB effects be understood. While numerous studies have demonstrated that GBs can influence QTL detection and estimation of effect sizes (Han
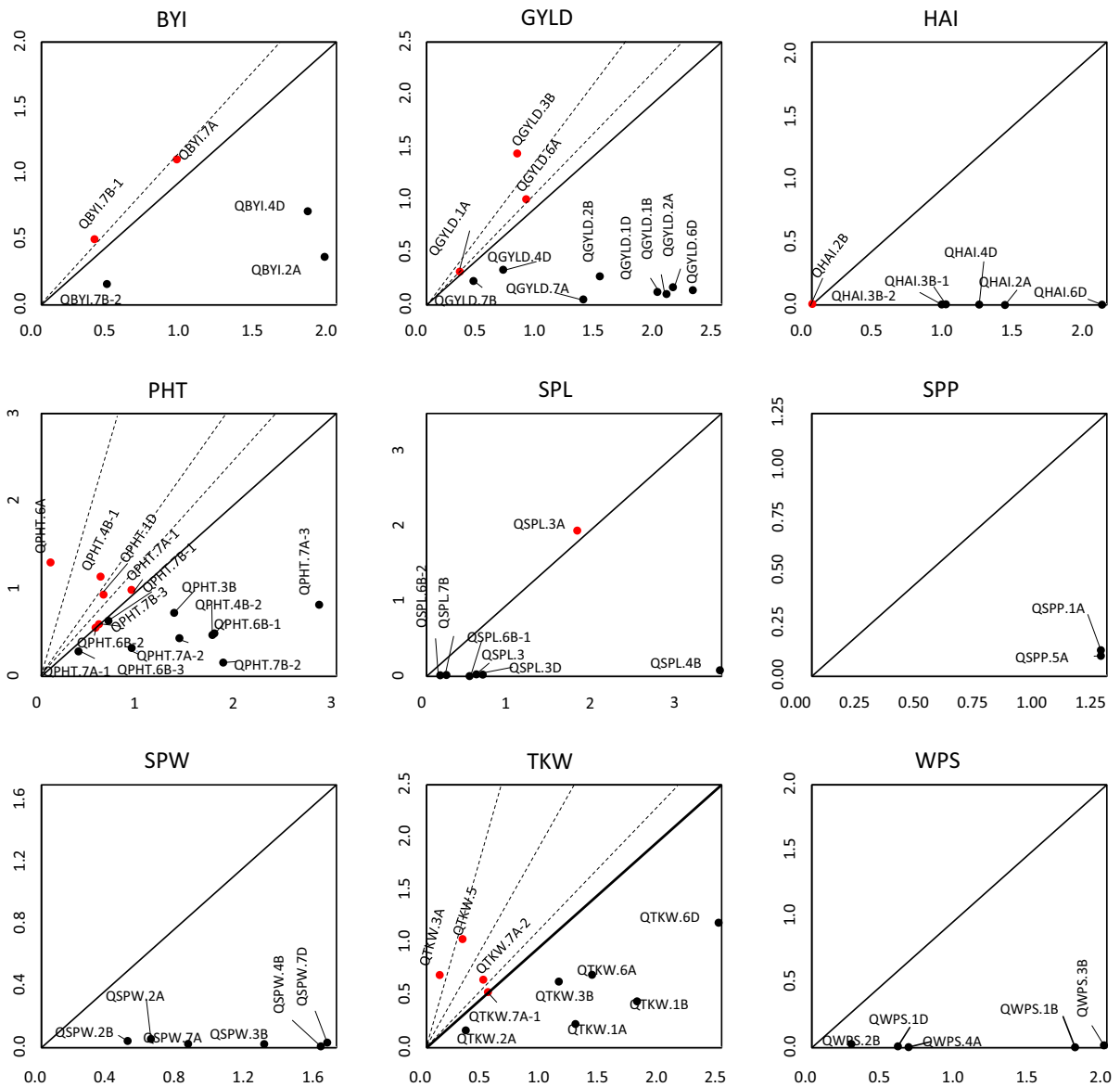
Fig. 2 Biplot analysis of QTL stability across environments, X: the first principal component scores (absolute value) of QTL by environment interaction effects, Y: main additive effect of QTLs (absolute value). QTLs under the thick line display larger QTL by environment interaction effects than main additive effects, whereas QTLs above the line demonstrate larger main additive effects than QTL by environment interaction effects (stable QTL across environment). The dotted lines and red dots highlight different levels of QTL stability and stable QTLs, respectively. (Color figure online)

et al. 2012; Wei et al. 2009; Yao et al. 2016), most studies still focus on QTLs underlying traits in a single population. The lack of repeatability of QTL effects across different genetic backgrounds (GB effect) and across environments (QEI effect) has limited the utilization of MAS in breeding (Price et al. 2002; Courtois et al. 2003; Lafitte et al. 2004; Bernier et al.

2008). Hence, the consistency of QTL effects in different GBs is a serious issue in marker-aided breeding projects.

Out of 92 reported M-QTLs in the present study by independent analyses of the three mapping populations across the three environments, only 2 ($\sim$ 5%) M-QTLs were identified in 2 genetic backgrounds in

Table 7 Joint analysis, comparison of genomic regions associated with yield-related and morphological traits in single and multi-environments

Trait	QTL	Pop[a]	ENV[b]	Chr.	Pos.	Marker interval	LOD	PVE[c] (%)	Add[d]	+Allele[e]
GYLD	QGYLD.1B	RF	Krl2	1B	180	wPt-320–wPt-6434	3.5866	3.4222	0.7028	Roshan
	QGYLD.2A-2	RF	Y11	2A	320	wPt-6687–wPt-729945	3.3546	7.9449	− 0.6110	Falat
	QGYLD.2A-1	RF	Krl2	2A	95	wPt-7187–wPt-115	3.0578	2.8703	0.4360	Roshan
	QGYLD.3D	RF	Krl3	3D	50	wPt-7241–wPt-730935	3.1998	3.6667	− 0.4490	Falat
	QGYLD.4D-1	RF	Krl2	4D	0	wPt-3058–wPt-672143	3.0529	2.6050	0.4492	Roshan
	QGYLD.4D-2	RSH	Krl3	4D	20	wPt-7769–wPt-665622	3.1595	4.4888	− 0.5595	Superhead#2
	QGYLD.6A-2	RF	Krl2	6A	160	wPt-228–wPt-741630	3.6348	4.5674	− 0.6482	Falat
	QGYLD.6A-1	RS	Krl3	6A	20	wPt-9589–wPt-653	3.9476	15.1472	− 1.0562	Sabalan
	QGYLD.6B	RS	Krl2	6B	95	wPt-494–wPt-741686	3.0253	45.1356	2.4571	Roshan
	QGYLD.1A	RS	Y11	1A	110	wPt-664968–wPt-5316	3.466	4.7872	0.3450	Roshan
	QGYLD.1D	RSH	Y11	1D	0	wPt-731338–wPt-667083	3.3204	5.4482	− 0.5941	Superhead#2
	QGYLD.2B	RF	Krl3	2B	300	wPt-6932–wPt-4301	3.4948	4.2513	0.4721	Roshan
	QGYLD.3B	RSH	Krl3	3B	160	wPt-731378–wPt-2559	3.8335	6.5998	− 0.6797	Superhead#2
	QGYLD.6A-3	RSH	Krl3	6A	380	wPt-5037–wPt-669672	3.7796	5.3191	0.6092	Roshan
	QGYLD.7A	RF	Y11	7A	225	wPt-4960–wPt-3523	3.9589	5.2413	0.5157	Roshan
	QGYLD.7B	RF	Krl3	7B	155	wPt-6484–wPt-6657	4.6688	5.4045	0.5331	Roshan
PHT	QPHT.1B	RF	Y11	1B	0	wPt-1070–wPt-734314	3.1013	3.6665	− 1.1017	Falat
	QPHT.2A	RF	Y11	2A	200	wPt-9277–wPt-1142	3.0361	5.1977	1.2699	Roshan
	QPHT.3D	RF	Krl2	3D	30	wPt-7241–wPt-730935	3.6870	17.3622	3.4077	Roshan
	QPHT.4B-1	RSH	Y11	4B	190	wPt-5390–wPt-4931	5.0280	9.7101	2.9625	Roshan
	QPHT.6A	RSH	Y11	6A	360	wPt-3778–wPt-3733	3.8608	7.3232	− 2.5705	Superhead#2
	QPHT.6B-1	RSH	Krl3	6B	20	wPt-7394–wPt-8166	3.6290	5.0224	− 1.3076	Superhead#2
	QPHT.6D-1	RS	Krl3	6D	315	wPt-7251–wPt-465	3.0662	3.6632	0.9148	Roshan
	QPHT.6D-2	RSH	Krl2	6D	415	wPt-7108–wPt-3226	3.4058	22.5462	− 9.6882	Superhead#2
	QPHT.1D	RSH	Y11	1D	165	wPt-3738–wPt-665480	3.8317	8.3126	2.7448	Roshan
	QPHT.3B	RF	Krl2	3B	365	wPt-669517–wPt-446	4.3793	5.9044	− 2.1957	Falat
	QPHT.4B-2	RSH	Krl3	4B	215	wPt-872–wPt-391	8.3622	16.1830	2.3401	Roshan
	QPHT.4B-3	RF	Krl2	4B	260	wPt-671760–wPt-5730	4.1320	5.1507	− 1.8533	Falat
	QPHT.6B-2	RF	Krl3	6B	190	wPt-669672–wPt-8554	4.2728	6.0601	− 1.4661	Falat
	QPHT.6B-3	RF	Y11	6B	355	wPt-4858–wPt-745128	4.6020	6.3632	1.3875	Roshan
	QPHT.6B-4	RF	Y11	6B	450	wPt-406–wPt-9952	3.5072	4.7324	1.2087	Roshan

Table 7 continued

Trait	QTL	Pop[a]	ENV[b]	Chr.	Pos.	Marker interval	LOD	PVE[c] (%)	Add[d]	+Allele[e]
	Single environment									
	QPHT.7A-1	RF	Krl3	7A	45	wPt-2260–wPt-741686	3.2447	4.7206	1.2984	Roshan
	QPHT.7A-2	RF	Krl3	7A	315	wPt-3992–wPt-3393	4.0100	6.1260	− 1.4368	Falat
	QPHT.7A-3	RSH	Krl3	7A	340	wPt-7925–wPt-8920	11.974	21.5644	3.1027	Roshan
	QPHT.7B	RF	Krl3	7B	155	wPt-6484–wPt-6657	13.7044	17.9018	2.4478	Roshan
SPL	QSPL.7B	RF	Krl3	7B	275	wPt-2305–wPt-3833	3.0644	3.7786	− 0.0373	Falat
	QSPL.7A	RF	Krl3	7A	305	wPt-4515–wPt-4744	3.2719	3.9020	− 0.0371	Falat
	QSPL.3B	RF	Krl2	3B	520	wPt-6802–wPt-5769	3.5016	3.3290	0.0729	Roshan
	QSPL.1B	RS	Y11	1B	55	wPt-734314–wPt-7259	3.0829	24.5325	− 0.4226	Sabalan
	QSPL.4A	RS	Y11	4A	310	wPt-672143–wPt-667538	3.2591	15.8203	0.2188	Roshan
	QSPL.5A	RS	Krl2	5A	65	tPt-8942–wPt-1505	3.9247	12.7455	0.7635	Roshan
	QSPL.3A	RSH	Krl2	3A	60	wPt-3389–wPt-664504	6.0098	42.9634	0.5083	Roshan
	QSPL.3D	RF	Krl2	3D	40	wPt-7241–wPt-730935	3.2706	5.7567	0.0934	Roshan
	QSPL.4B	RF	Krl2	4B	260	wPt-671760–wPt-5730	37.1734	39.0704	− 0.2410	Falat
	QSPL.6B	RF	Krl3	6B	175	wPt-9124–wPt-1730	5.0646	6.2210	0.0481	Roshan
TKW	QTKW.3A-2	RF	Krl2	3A	220	wPt-9761–wPt-6422	3.0145	3.9299	− 0.9558	Falat
	QTKW.1B-1	RF	Krl3	1B	140	wPt-6012–wPt-3451	3.1680	4.3216	1.2318	Roshan
	QTKW.5D	RF	Krl2	5D	40	wPt-5505–wPt-2256	4.6804	6.5939	1.4917	Roshan
	QTKW.3A-1	RS	Krl3	3A	75	wPt-8699–wPt-733571	3.6193	5.7961	− 1.6934	Sabalan
	QTKW.3B-2	RSH	Krl2	3B	365	wPt-3094–wPt-7212	3.7615	7.8024	− 1.9404	Superhead#2
	QTKW.1A	RSH	Y11	1A	95	wPt-668205–wPt-664666	5.9067	14.8009	1.7732	Roshan
	QTKW.1B-2	RF	Y11	1B	270	wPt-1248–wPt-9857	3.2682	5.1372	− 1.5757	Falat
	QTKW.2A	RF	Krl3	2A	95	wPt-7187–wPt-115	3.1329	4.3304	1.2225	Roshan
	QTKW.3B-1	RF	Krl2	3B	365	wPt-669517–wPt-446	5.5150	8.1435	− 1.4917	Falat
	QTKW.5B	RSH	Krl3	5B	0	wPt-1400–wPt-663848	14.4912	33.0543	4.2248	Roshan
	QTKW.6A	RSH	Krl2	6A	310	wPt-6282–wPt-7954	3.9683	7.0318	− 1.8162	Superhead#2
	QTKW.7A	RSH	Krl3	7A	335	wPt-664218–wPt-7925	3.2871	4.4880	1.5285	Roshan

Table 7 continued

Trait	QTL	LOD	PVE^c (%)	Add^d	A*KR13^f	A*KR12^g	A*Y11^h	Stable
GYLD	–	–	–	–	–	–	–	Specific for Krl2
	–	–	–	–	–	–	–	Specific for Y11
	–	–	–	–	–	–	–	Specific for Krl2
	–	–	–	–	–	–	–	Specific for Krl3
	–	–	–	–	–	–	–	Specific for Krl2
	–	–	–	–	–	–	–	Specific for Krl3
	–	–	–	–	–	–	–	Specific for Krl2
	–	–	–	–	–	–	–	Specific for Krl3
	–	–	–	–	–	–	–	Specific for Krl2
	QGYLD.1A	3.3681	0.6790	0.3171	− 0.0990	0.0286	0.0704	Environmentally stable
	QGYLD.1D	3.5092	1.3156	− 0.1239	0.4675	− 0.0781	− 0.3893	Specific for Y11
	QGYLD.2B	4.1887	1.9550	0.2723	0.1929	0.0386	− 0.2315	Specific for Krl3
	QGYLD.3B	3.2977	2.1916	− 1.4406	− 0.1180	− 0.1672	0.2852	Environmentally stable
	QGYLD.6A	3.5002	1.3246	1.0058	0.3094	− 0.1778	− 0.1316	Environmentally stable
	QGYLD.7A	3.8222	1.6260	0.0528	− 0.008	− 0.3657	0.3736	Specific for Y11
	QGYLD.7B	3.2376	1.4154	0.2281	0.1987	− 0.1810	− 0.0178	Specific for Krl3
PHT	–	–	–	–	–	–	–	Specific for Y11
	–	–	–	–	–	–	–	Specific for Y11
	–	–	–	–	–	–	–	Specific for Krl2
	–	–	–	–	–	–	–	Specific for Y11
	–	–	–	–	–	–	–	Specific for Y11
	–	–	–	–	–	–	–	Specific for Krl3
	–	–	–	–	–	–	–	Specific for Krl3
	–	–	–	–	–	–	–	Specific for Krl2
	QPHT.1D	3.9063	1.8617	0.9329	− 0.4496	− 0.7473	1.1969	Environmentally stable
	QPHT.3B	4.1162	2.2987	− 0.725	0.7015	− 1.1724	0.4709	Specific for Krl2
	QPHT.4B-1	3.2114	1.6655	1.1381	− 0.1734	− 0.3341	0.5075	Environmentally stable
	QPHT.4B-2	4.7081	2.7172	− 0.4722	0.8581	− 1.3681	0.5101	Specific for Krl2
	QPHT.6B-1	3.4437	1.1552	− 0.4909	− 0.7178	0.1222	0.5956	Specific for Krl3
	QPHT.6B-2	3.5841	1.0426	0.5554	− 0.1572	− 0.3664	0.5236	Environmentally stable
	QPHT.6B-3	3.2527	0.6568	0.3236	− 0.3513	− 0.2563	0.6076	Specific for Y11

Table 7 continued

| Trait | Multi environments | | | | | | | |
	QTL	LOD	PVE^c (%)	Add^d	A*KR13^f	A*KR12^g	A*Y11^h	Stable
	QPHT.7A-2	3.2451	0.6869	0.2848	0.6518	− 0.1272	− 0.5246	Specific for Kr13
	QPHT.7A-3	3.8883	0.9107	− 0.4358	− 0.5514	− 0.0196	0.5711	Specific for Kr13
	QPHT.7A-4	5.6119	2.1817	0.8172	1.3470	− 1.8312	0.4842	Specific for Kr13
	QPHT.7B-2	4.7046	1.9508	0.1575	1.0692	− 1.1531	0.0839	Specific for Kr13
SPL	–	–	–	–	–	–	–	Specific for Kr13
	–	–	–	–	–	–	–	Specific for Kr13
	–	–	–	–	–	–	–	Specific for Kr12
	–	–	–	–	–	–	–	Specific for Y11
	–	–	–	–	–	–	–	Specific for Y11
	–	–	–	–	–	–	–	Specific for Kr12
	QSPL.3A	3.2165	3.9128	1.9409	− 0.0508	0.0891	− 0.0382	Environmentally stable
	QSPL.3D	3.2154	1.8291	0.0232	− 0.0199	0.0385	− 0.0186	Specific for Kr12
	QSPL.4B	36.4194	26.5693	− 0.0812	0.0683	− 0.1485	0.0802	Specific for Kr12
	QSPL.6B-1	3.6102	0.6263	0.0182	0.0136	− 0.0021	− 0.0115	Specific for Kr13

Table 7 continued

Trait	Multi environments								
	QTL	LOD	PVE[c] (%)	Add[d]	A*KR13[f]	A*KR12[g]	A*Y11[h]	Stable
TKW	–	–	–	–	–	–	–	Specific for Kr12
	–	–	–	–	–	–	–	Specific for Kr13
	–	–	–	–	–	–	–	Specific for Kr12
	–	–	–	–	–	–	–	Specific for Kr13
	–	–	–	–	–	–	–	Specific for Kr12
	QTKW.1A	3.0471	0.7860	0.2257	– 0.4111	– 0.2867	0.6978	Specific for Y11
	QTKW.1B	3.0795	1.0498	– 0.4412	0.5166	0.4464	– 0.9631	Specific for Y11
	QTKW.2A	3.8486	2.0621	0.1652	0.9964	– 0.6650	– 0.3314	Specific for Kr13
	QTKW.3B	4.3754	1.9459	– 0.6292	– 0.1383	– 0.4427	0.5809	Specific for Kr12
	QTKW.5B	3.7864	2.9028	1.0335	0.6782	– 0.4156	– 0.2626	Environmentally stable
	QTKW.6A	3.7591	2.3953	– 0.6938	0.2411	– 0.8950	0.6538	Specific for Kr12
	QTKW.7A-2	3.7414	2.9324	0.6474	1.1024	– 1.1525	0.0502	Environmentally stable

Min. minimum, *Max.* maximum, *SD* standard deviation, *PHT* plant height, *SPL* spike length, *SPW* spike weight, *WKP* weight of kernels in plant, *TKW* thousand kernel weight, *SPP* spike per plant, *GYLD* grain yield per plant, *BYI* biological yield per m², *HAI* harvest index, *RF* Roshan*Falat, *RS* Roshan*Sabalan, *RSH* Roshan*Superhead#2, *KR13* Kerman-2013, *KR12* Kerman-2012, *Y11* Yazd-2011

[a]Mapping population for detected QTL

[b]The environment of detected QTL

[c]Phenotypic variation explained

[d]Additive effect of detected QTL

[e]Source of positive allele

[f]Additive by Environment (Kerman-2013) effect

[g]Additive by Environment (Kerman-2012) effect

[h]Additive by Environment (Yazd-2011) effect

the same environment. Surprisingly, joint analyses failed to detect QTLs common to all 3 genetic backgrounds. This finding demonstrates the GB-specific effect of QTLs for yield-related traits under salinity stress. These findings are generally consistent with previous research. For example, Cui et al. (2014) reported that 7–36% of QTLs were shared across 2–3 wheat genetic backgrounds. Thus, it is clear that genetic background plays a large role in the expression of QTLs for salinity tolerance, and yield-related MAS for salt tolerance must take the genetic backgrounds of breeding populations into account.

Epistatic interactions

Fully understanding the impact of epistasis on quantitative traits remains a key challenge (Le Rouzic and Álvarez-Castro 2008). In a detailed investigation into epistatic effects on wheat grain yield, Reif et al. (2011) concluded that exploitation of epistasis is key to increased selection gain via marker-assisted breeding. To elucidate the possible epistatic interaction effects of detected M-QTLs in the independent analysis, all possible effects were calculated based on 5 cM windows. A total of 191 epistatic interactions were found. Of these, only 3 co-localized with M-QTLs. The majority of the interacting loci have no significant main additive effects, similar to previous reports from wheat (Reif et al. 2011), barley (Xu and Jia 2007), rice (Li et al. 1997), humans (Nyholt et al. 2008), drosophila (Montooth et al. 2003) and mice (Leamy et al. 2005). Epistatic interactions involving the 3 M-QTLs alluded to above explained 25 to 37% of PVE. Interestingly, most of the epistatic interactions had a negative effect on traits, possibly implying that recombination in the mapping populations has disrupted favorable gene complexes.

QTL analysis in single and multi-environments

Previous studies of genetic responses to salt stress also indicate that the identification and expression of many QTLs is environment dependent. Environmental variation can result in changes in the magnitude and direction of QTL effects, leading to inconsistency in QTL detection, as well apparent reductions in LOD scores (Villalta et al. 2007; Xue et al. 2009). Inconsistency in QTL detection across multiple environments could be attributable to differing levels of stress experienced by the mapping population. Azadi et al. (2015) conducted research on QTL mapping of yield and yield components under normal and salt stress conditions in bread wheat. They recommended analyses of QTL by environment interactions as a means of accounting for inconsistent detection of QTLs between environments.

A better understanding of QTL by environment effects under salinity stress would lead to progress in wheat salinity tolerance breeding. Hence, QTL stability across multiple environments is key to developing a successful marker-aided breeding strategy. QTL mapping for yield-related traits across environments has previously been reported (Quarrie et al. 2006; Zhang et al. 2010; Azadi et al. 2015; Liu et al. 2014; Guan et al. 2018; Gao et al. 2015; Wu et al. 2015; Würschum et al. 2015; Nadolska-Orczyk et al. 2017; Shi et al. 2017). In the present study, a total of 67 QTLs associated with yield-related and morphological traits were identified across multiple environments (Table 6).

One of the most important morphological traits of wheat is plant height, since a significant gain in wheat yield occurred through the introduction of reduced height (Rht) dwarfing genes (Hedden 2003; Zhang et al. 2006). As shown in the biplots the 15 QTLs for plant height range from unstable to relatively stable across environments (Fig. 2). As shown in joint analyses QPHT.6A, QPHT.4B-1, QPHT.1D, QPHT.7A-1, QPHT.7B-3 and QPHT.6B-2 had the highest QTL stability (Fig. 2) and have previously been identified in other QTL mapping studies (Gao et al. 2015; Klahr et al. 2007; Huang et al. 2003; Zhang et al. 2010). QPHT.4B-1 and QPHT.1D were also detected as M-QTLs in the RSH population with the beneficial allele derived from Roshan. These QTLs explained 16.1 and 8.3 percent of PHT variation, respectively. As shown in the joint genotype by environment analyses, nine QTLs were unstable across environments.

A total of 10 QTLs were identified for thousand kernel weight across environments in the three mapping populations. Joint genotype by environment analyses identified four QTLs (QTKW.3A, QTKW.5B, QTKW.7A-1, QTKW.7A-2) showing the greatest stability across environments. These results match those observed in earlier studies. Groos et al. (2003) in a detailed genetic analysis of TKW reported QTLs on chromosome 5B and 7A in 7

environments. They also found another QTL on chromosome 3A in a single environment, suggesting that it was unstable.

The ever-growing global population and limited agricultural land make the development of high-yielding varieties an absolute priority for wheat breeders (Lobell et al. 2011; Ray et al. 2012). Therefore, the identification and validation of yield-related QTLs can facilitate improvement of high-yielding varieties. In the present study, joint genotype by environment analyses revealed that QGYLD.3B, QGYLD.6A, QGYLD.1A were the most stable QTLs for GYLD (Fig. 2). As expected, the beneficial allele in 2 out of 3 stable QTLs associated with GYLD were derived from Roshan (high yield and salinity tolerant parent). These QTLs have been reported in previous studies (Groos et al. 2003; Huang et al. 2003; Azadi et al. 2015; Zhang et al. 2010). A single stable QTL (QHAI.2B) out of 6 was identified for HAI. Kumar et al. (2007) also found a QTL for harvest index in Chromosome 2B of wheat. As clear in the biplot analysis there were no stable QTLs for SPP, SPW and WKP (Fig. 2), although several M-QTLs were detected for SPP, SPW and WKP in single environments. MAS should be applied with caution for such environment-specific QTLs.

Among the 7 identified QTLs for spike length, QSPL.3A showed a stable pattern across environments, as did QSPL.3A, which was the most stable QTL associated with SPL. To the best of our knowledge, the most stable quantitative trait loci for SPL (QSPL.3A) has not previously been reported. This novel QTL was identified in the RSH population with the positive allele derived from Roshan.

Two stable QTLs (QBYI.7A and QBYI.7B-1) were detected for biological yield (Fig. 2). QTL on chromosome 7A were previously reported for BYI (Sardouie-Nasab et al. 2013; Kumar et al. 2007). As far as we are aware, QBYI.7B-1, which is the most stable QTL for BYI detected in this study, has not previously been reported. Notably, the beneficial allele of QBYI.7B-1 was derived from Roshan.

In conclusion, we carried out QTL mapping for yield-related and morphological traits of wheat, with the aim of identifying QTLs under salinity stress and their effects in different genetic backgrounds, as well as their epistatic and environmental interactions. Overall, in the independent analysis, we detected 92 putative M-QTLs associated with 9 different yield-related and morphological traits. Whereas 191 epistatic QTLs were detected, only 3 epistatic QTLs involved M-QTLs. While we found seventeen environmentally stable QTLs for biological yield, grain yield, harvest index, plant height, spike length, and thousand kernel weight, only 4 QTLs were found across two genetic backgrounds and none across three. Genetic background independent QTLs with environmental stability will be most valuable for designing marker-assisted selection schemes in diverse environments. In the future it will be important to move beyond bi-parental mapping populations to genome-wide association analyses using very large numbers of SNP markers, with the goal of enabling genomic selection for salt tolerance in wheat.

Ultimately, these findings have important implications for developing marker-assisted selection strategies for wheat breeding under salinity stress. The consistent effect of highly stable QTLs across different environments offers great opportunities for further functional genomics analysis to characterize genes for improving wheat yield under salinity stress.

References

Akbari M, Wenzl P, Caig V, Carling J, Xia L, Yang S, Uszynski G, Mohler V, Lehmensiek A, Kuchel H (2006) Diversity arrays technology (DArT) for high-throughput profiling of the hexaploid wheat genome. Theor Appl Genet 113(8):1409–1420

Azadi A, Mardi M, Hervan EM, Mohammadi SA, Moradi F, Tabatabaee MT, Pirseyedi SM, Ebrahimi M, Fayaz F, Kazemi M (2015) QTL mapping of yield and yield components under normal and salt-stress conditions in bread wheat (*Triticum aestivum* L.). Plant Mol Biol Report 33(1):102–120

Bernier J, Atlin GN, Serraj R, Kumar A, Spaner D (2008) Breeding upland rice for drought resistance. J Sci Food Agric 88(6):927–939

Budak H, Shearman R, Parmaksiz I, Gaussoin R, Riordan T, Dweikat I (2004) Molecular characterization of buffalo-grass germplasm using sequence-related amplified polymorphism markers. Theor Appl Genet 108(2):328–334

Castillo A, Budak H, Varshney RK, Dorado G, Graner A, Hernandez P (2008) Transferability and polymorphism of barley EST-SSR markers used for phylogenetic analysis in Hordeum chilense. BMC Plant Biol 8(1):97

Courtois B, Shen L, Petalcorin W, Carandang S, Mauleon R, Li Z (2003) Locating QTLs controlling constitutive root traits in the rice population IAC 165 × Co39. Euphytica 134(3):335–345

Cui F, Zhao C, Ding A, Li J, Wang L, Li X, Bao Y, Li J, Wang H (2014) Construction of an integrative linkage map and QTL mapping of grain yield-related traits using three related wheat RIL populations. Theor Appl Genet 127(3):659–675

Cui T, He K, Chang L, Zhang X, Xue J, Liu J (2017) QTL mapping for leaf area in maize (Zea mays L.) under multi-environments. J Integr Agric 16(4):800–808

Dehdari A, Rezai A, Maibody SAM (2005) Salt tolerance of seedling and adult bread wheat plants based on ion contents and agronomic traits. Commun Soil Sci Plant Anal 36(15–16):2239–2253

FAO (2018) Online statistical database: food balance. Food and Agricultural Organization of the United Nations. Available online at http://www.fao.org/faostat/en/

Flowers T, Flowers S (2005) Why does salinity pose such a difficult problem for plant breeders? Agric Water Manag 78(1–2):15–24

Flowers T, Yeo A (1995) Breeding for salinity resistance in crop plants: where next? Funct Plant Biol 22(6):875–884

Gao F, Wen W, Liu J, Rasheed A, Yin G, Xia X, Wu X, He Z (2015) Genome-wide linkage mapping of QTL for yield components, plant height and yield-related physiological traits in the Chinese wheat cross Zhou 8425B/Chinese Spring. Front Plant Sci 6:1099

Groos C, Robert N, Bervas E, Charmet G (2003) Genetic analysis of grain protein-content, grain yield and thousand-kernel weight in bread wheat. Theor Appl Genet 106(6):1032–1040

Guan P, Lu L, Jia L, Kabir MR, Zhang J, Zhao Y, Xin M, Hu Z, Yao Y, Ni Z (2018) Global QTL analysis identifies genomic regions on chromosomes 4A and 4B harboring stable loci for yield-related traits across different environments in wheat (Triticum aestivum L.). Front Plant Sci 9:529

Han Y, Li D, Zhu D, Li H, Li X, Teng W, Li W (2012) QTL analysis of soybean seed weight across multi-genetic backgrounds and environments. Theor Appl Genet 125(4):671–683

Hedden P (2003) The genes of the green revolution. Trends Genet 19(1):5–9

Huang X, Cöster H, Ganal M, Röder M (2003) Advanced backcross QTL analysis for the identification of quantitative trait loci alleles from wild relatives of wheat (Triticum aestivum L.). Theor Appl Genet 106(8):1379–1389

Hussain B (2015) Modernization in plant breeding approaches for improving biotic stress resistance in crop plants. Turk J Agric For 39(4):515–530

Jahani M, Nematzadeh G, Dolatabadi B, Hashemi SH, Mohammadi-Nejad G (2014) Identification and validation of functional markers in a global rice collection by association mapping. Genome 57(6):355–362

Klahr A, Zimmermann G, Wenzel G, Mohler V (2007) Effects of environment, disease progress, plant height and heading date on the detection of QTLs for resistance to Fusarium head blight in an European winter wheat cross. Euphytica 154(1–2):17–28

Kosambi DD (1943) The estimation of map distances from recombination values. Ann Eugen 12(1):172–175

Kumar N, Kulwal P, Balyan H, Gupta P (2007) QTL mapping for yield and yield contributing traits in two mapping populations of bread wheat. Mol Breed 19(2):163–177

Lafitte H, Ismail A, Bennett J (2004) Abiotic stress tolerance in rice for Asia: progress and the future. In: Fischer T, Turner N, Angus J, McIntyre L, Robertson M, Borrell A (eds) New directions for a diverse planet: proceedings of the 4th international crop science congress. Brisbane, Australia

Le Rouzic A, Álvarez-Castro JM (2008) Estimation of genetic effects and genotype-phenotype maps. Evolut Bioinform 4:EBO-S756

Leamy L, Workman M, Routman E, Cheverud J (2005) An epistatic genetic basis for fluctuating asymmetry of tooth size and shape in mice. Heredity 94(3):316

Li ZK, Pinson S, Park W (1997) Epistasis for three grain yield components in rice (Oryza sativa L.). Genetics 145(2):453–465

Li H, Ribaut J-M, Li Z, Wang J (2008) Inclusive composite interval mapping (ICIM) for digenic epistasis of quantitative traits in biparental populations. Theor Appl Genet 116(2):243–260

Li S, Wang J, Zhang L (2015) Inclusive composite interval mapping of QTL by environment interactions in biparental populations. PLoS ONE 10(7):e0132414

Liu G, Jia L, Lu L, Qin D, Zhang J, Guan P, Ni Z, Yao Y, Sun Q, Peng H (2014) Mapping QTLs of yield-related traits using RIL population derived from common wheat and Tibetan semi-wild wheat. Theor Appl Genet 127(11):2415–2432

Lobell DB, Schlenker W, Costa-Roberts J (2011) Climate trends and global crop production since 1980. Science 333(6042):616–620

Mathews KL, Malosetti M, Chapman S, McIntyre L, Reynolds M, Shorter R, van Eeuwijk F (2008) Multi-environment QTL mixed models for drought stress adaptation in wheat. Theor Appl Genet 117(7):1077–1091

McFarland ML, Provin TL, Redmon LA, Boellstorff DE, McDonald AK, Stein LA, Wherley BG (2014) An index of salinity and boron tolerance of common native and introduced plant species in Texas. Texas A&M Agrilife Extension Service College Station, Texas

Montooth KL, Marden JH, Clark AG (2003) Mapping determinants of variation in energy metabolism, respiration and flight in Drosophila. Genetics 165(2):623–635

Munns R, James RA, Läuchli A (2006) Approaches to increasing the salt tolerance of wheat and other cereals. J Exp Bot 57(5):1025–1043

Nadolska-Orczyk A, Rajchel IK, Orczyk W, Gasparis S (2017) Major genes determining yield-related traits in wheat and barley. Theor Appl Genet 130(6):1081–1098

Nyholt DR, LaForge KS, Kallela M, Alakurtti K, Anttila V, Färkkilä M, Hämäläinen E, Kaprio J, Kaunisto MA, Heath AC (2008) A high-density association screen of 155 ion transport genes for involvement with common migraine. Hum Mol Genet 17(21):3318–3331

Poustini K, Siosemardeh A (2004) Ion distribution in wheat cultivars in response to salinity stress. Field Crops Res 85(2–3):125–133

Prashant R, Kadoo N, Desale C, Kore P, Dhaliwal HS, Chhuneja P, Gupta V (2012) Kernel morphometric traits in hexaploid wheat (Triticum aestivum L.) are modulated by intricate

QTL × QTL and genotype × environment interactions. J Cereal Sci 56(2):432–439

Price AH, Cairns JE, Horton P, Jones HG, Griffiths H (2002) Linking drought-resistance mechanisms to drought avoidance in upland rice using a QTL approach: progress and new opportunities to integrate stomatal and mesophyll responses. J Exp Bot 53(371):989–1004

Quarrie S, Pekic Quarrie S, Radosevic R, Rancic D, Kaminska A, Barnes J, Leverington M, Ceoloni C, Dodig D (2006) Dissecting a wheat QTL for yield present in a range of environments: from the QTL to candidate genes. J Exp Bot 57(11):2627–2637

Ray DK, Ramankutty N, Mueller ND, West PC, Foley JA (2012) Recent patterns of crop yield growth and stagnation. Nat Commun 3:1293

Rebetzke GJ, Ellis MH, Bonnett DG, Richards RA (2007) Molecular mapping of genes for Coleoptile growth in bread wheat (*Triticum aestivum* L.). Theor Appl Genet 114(7):1173–1183. https://doi.org/10.1007/s00122-007-0509-1

Reif JC, Maurer HP, Korzun V, Ebmeyer E, Miedaner T, Würschum T (2011) Mapping QTLs with main and epistatic effects underlying grain yield and heading time in soft winter wheat. Theor Appl Genet 123(2):283

Saade S, Maurer A, Shahid M, Oakey H, Schmöckel SM, Negrão S, Pillen K, Tester M (2016) Yield-related salinity tolerance traits identified in a nested association mapping (NAM) population of wild barley. Sci Rep 6:32586

Sardouie-Nasab S, Mohammadi-Nejad G, Zebarjadi A (2013) Haplotype analysis of QTLs attributed to salinity tolerance in wheat (*Triticum aestivum*). Mol Biol Rep 40(7):4661–4671

Shi W, Hao C, Zhang Y, Cheng J, Zhang Z, Liu J, Yi X, Cheng X, Sun D, Xu Y (2017) A combined association mapping and linkage analysis of kernel number per spike in common wheat (*Triticum aestivum* L.). Front Plant Sci 8:1412

Venuprasad R, Bool M, Quiatchon L, Atlin G (2012) A QTL for rice grain yield in aerobic environments with large effects in three genetic backgrounds. Theor Appl Genet 124(2):323–332

Vikram P, Swamy BM, Dixit S, Ahmed HU, Cruz MTS, Singh AK, Kumar A (2011) qDTY 1.1, a major QTL for rice grain yield under reproductive-stage drought stress with a consistent effect in multiple elite genetic backgrounds. BMC Genet 12(1):89

Villalta I, Bernet G, Carbonell E, Asins M (2007) Comparative QTL analysis of salinity tolerance in terms of fruit yield using two solanum populations of F 7 lines. Theor Appl Genet 114(6):1001–1017

Wang X, Pang Y, Zhang J, Zhang Q, Tao Y, Feng B, Zheng T, Xu J, Li Z (2014) Genetic background effects on QTL and QTL × environment interaction for yield and its component traits as revealed by reciprocal introgression lines in rice. Crop J 2(6):345–357

Wei M, Fu J, Li X, Wang Y, Li Y (2009) Influence of dent corn genetic backgrounds on QTL detection for plant-height traits and their relationships in high-oil maize. J Appl Genet 50(3):225–234

Wenzl P, Carling J, Kudrna D, Jaccoud D, Huttner E, Kleinhofs A, Kilian A (2004) Diversity Arrays Technology (DArT) for whole-genome profiling of barley. Proc Natl Acad Sci USA 101(26):9915–9920

Wu Q-H, Chen Y-X, Zhou S-H, Fu L, Chen J-J, Xiao Y, Zhang D, Ouyang S-H, Zhao X-J, Cui Y (2015) High-density genetic linkage map construction and QTL mapping of grain shape and size in the wheat population Yanda 1817 × Beinong6. PLoS ONE 10(2):e0118144

Würschum T, Langer SM, Longin CFH (2015) Genetic control of plant height in European winter wheat cultivars. Theor Appl Genet 128(5):865–874

Xu S, Jia Z (2007) Genomewide analysis of epistatic effects for quantitative traits in barley. Genetics 175(4):1955–1963

Xue D, Huang Y, Zhang X, Wei K, Westcott S, Li C, Chen M, Zhang G, Lance R (2009) Identification of QTLs associated with salinity tolerance at late growth stage in barley. Euphytica 169(2):187–196

Yao X, Wang J, Jin L, Wei W, Yang S, Zhang Y, Xu Z (2016) Comparison and analysis of QTLs for grain and hull thickness related traits in two recombinant inbred line (RIL) populations in rice (*Oryza sativa* L.). J Integr Agric 15(11):2437–2450

Zhang X, Yang S, Zhou Y, He Z, Xia X (2006) Distribution of the Rht-B1b, Rht-D1b and Rht8 reduced height genes in autumn-sown Chinese wheats detected by molecular markers. Euphytica 152(1):109–116

Zhang K, Tian J, Zhao L, Wang S (2008) Mapping QTLs with epistatic effects and QTL × environment interactions for plant height using a doubled haploid population in cultivated wheat. J Genet Genom 35(2):119–127

Zhang LY, Liu DC, Guo XL, Yang WL, Sun JZ, Wang DW, Zhang A (2010) Genomic distribution of quantitative trait loci for yield and yield-related traits in common wheat. J Integr Plant Biol 52(11):996–1007

Zheng BS, Le Gouis J, Leflon M, Rong WY, Laperche A, Brancourt-Hulmel M (2010) Using probe genotypes to dissect QTL × environment interactions for grain yield components in winter wheat. Theor Appl Genet 121(8):1501–1517